Hydrogen-bonding configuration effects on the optoelectronic properties of glow discharge a-$Si_{1-x}Ge_x$:H with large x

2007 J. Phys.: Condens. Matter 19 356215

(http://iopscience.iop.org/0953-8984/19/35/356215)

IOP PUBLISHING JOURNAL OF PHYSICS: CONDENSED MATTER

J. Phys.: Condens. Matter **19** (2007) 356215 (14pp) doi:10.1088/0953-8984/19/35/356215

Hydrogen-bonding configuration effects on the optoelectronic properties of glow discharge a-$Si_{1-x}Ge_x$:H with large x

Y Bouizem, A Belfedal[1], J D Sib, A Kebab and L Chahed

Laboratoire de Physique des Couches Minces et Matériaux pour l'Electronique, Université d'Oran, Es-Sénia 31100, Algeria

E-mail: a_belfedal@hotmail.com

Received 29 May 2007
Published 8 August 2007
Online at stacks.iop.org/JPhysCM/19/356215

Abstract

The optical and structural properties of hydrogenated amorphous silicon–germanium (a-$Si_{1-x}Ge_x$:H) films, deposited at high growth rate by radio-frequency (RF) glow discharge on the powered electrode in a conventional parallel plate reactor, were investigated by infrared transmission measurements, standard optical transmission measurements and the photothermal deflection spectroscopy (PDS) method. By varying the electrode gap spacing, D, from 3.2 to 0.8 cm, and keeping all others parameters of the plasma constant, a gradual change in the hydrogen-bonding configurations was observed. The effects of this change on the structure of the material, on the optical gap, and on the midgap density are investigated and discussed at high fixed composition ($x = 0.8$) and at constant total bonded hydrogen content (C_H(at.%) $= 8.5$). The optical gaps (1.16 eV $\leqslant E_T \leqslant$ 1.22 eV) of the films are less than those of conventional films, reported in the literature. The level of absorption at energies bellow the Urbach tail decreases with D and reaches an optimum at $D = 0.8$ cm. The disorder parameter ($E_{0v} \approx 46 \pm 1$ meV) and the level of absorption in optimized samples are of the same order as those of device-quality a-Si:H films. It is suggested that the remarkable improvement of the electronic properties of the alloys is mainly due to the incorporation of the hydrogen in the bulk of the material as Ge–H and Si–H bonds, with a preferential attachment to Ge rather than to both Ge and Si.

1. Introduction

For more than a decade, hydrogenated amorphous silicon–germanium (a-$Si_{1-x}Ge_x$:H) alloys have received much interest [1–3], especially because this material has various promising applications in solar cells [4, 5]. Alloying hydrogenated amorphous silicon (a-Si:H) with

[1] Author to whom any correspondence should be addressed.

Ge narrows the optical bandgap of the material [6], allowing it to absorb photons from less energetic portions of the solar spectrum. Usually a semiconductor with a bandgap near 1.4 eV is considered optimum for use in the bottom layer of a tandem cell [7, 8]. However, it is now widely recognized that there is a sharp deterioration of the electronic properties of this binary alloy with an increasing Ge content [9, 10]. This is often attributed to an increase in the number of recombination centres, mainly due to the preferential attachment of hydrogen to silicon [11, 13]. This had led to a great deal of research work to improve the optoelectronic properties of the alloy. Many deposition processes have been explored [12, 14], but the trend of deterioration with increasing Ge content has persisted. So, instead of approaching the a-$Si_{1-x}Ge_x$:H film deposition problem as a perturbation of the standard conditions which lead to device-quality a-Si:H, many authors [15, 16] have suggested that the photo-response of a-$Si_{1-x}Ge_x$:H alloys can be improved through the optimization of the deposition methods leading to high electronic quality a-Ge:H films, and through proper understanding of their properties. Following this idea, many researchers were able to deposit high structural quality a-Ge:H films by the plasma-enhanced chemical vapour deposition (PECVD) technique on the powered electrode (cathode) of the reactor [17, 18]. The optimized deposition conditions for this material were very different from those of device-quality a-Si:H, but their optoelectronic properties were much improved over that previously obtained on the unpowered electrode (anode) [17]. Also, in a recent study, we have reported on the effect of the radio-frequency (RF) power on the optoelectronic properties of a-Ge:H films deposited by the PECVD technique on the powered electrode [19]. In particular, we have shown that, by operating the discharge in the high-pressure and the high RF power regime, we could increase the deposition rate up to 10 Å s^{-1}. The disorder parameters were equal to 44 ± 2 meV, but the deep-gap state density was roughly at an order of magnitude higher than in optimized a-Si:H.

The results presented in this paper extend this work. We report on the optoelectronic properties of a-$Si_{1-x}Ge_x$:H alloys deposited at high growth rate, under the same conditions of the plasma leading to optimized a-Ge:H films [19]. We examine in particular the effects of the hydrogen-bonding configurations on the structure of the material, on the optical gap, and on the midgap density. These parameters are investigated at high fixed composition $x = 0.8$ (determined by electron microprobe measurements), and at constant total bonded hydrogen content, C_H(at.%).

2. Experimental details

The a-$Si_{1-x}Ge_x$:H samples were deposited by the RF-PECVD technique at 13.56 MHz in the reactor described elsewhere in the literature [18], from SiH_4 (2 sccm)/GeH_4(0.8 sccm)/H_2 (20 sccm) mixture. In order to maintain the composition x and C_H(at.%) constant for all the samples, the gas flows, the substrate temperature ($T_s = 200\,^{\circ}C$) and the chamber pressure ($P = 0.95$ Torr) were kept constant. The samples were deposited on the cathode (diameter $= 5.7$ cm) at 30 W of RF power and at different values of the electrode gap, D, ranging from 3.2 to 0.8 cm. This electrode acquires a negative self-bias voltage, V_b, with respect to the potential plasma (at $D = 3.2$ cm, V_b is nearly equal to -120 V and decreases to -100 V at $D = 0.8$ cm) and is therefore subject to more or less ion bombardment. As V_b is directly related to the electrode gap we shall argue that ion bombardment and the electric field between the electrodes may play a dominant role in explaining the differences which can be observed between the samples.

The optical absorption spectra, $\alpha(\hbar\omega)$, for energies lower than the optical gap were determined accurately down to 0.6 eV, by a combination of standard optical transmission measurements and the photothermal deflexion spectroscopy (PDS) method [20], performed on

the same samples deposited on Corning 7059 glass substrates. By comparing the data obtained on series of samples deposited under the same conditions but with different thicknesses, we checked that in all cases the surface absorptions were negligible for thicknesses in the 1–3 μm range. The analysis of the optical transmission spectra allows us to determine the optical gap, E_T, and from the interference fringes, the thickness, d, and the refractive index $n(\lambda)$. The characteristic parameter of the disorder, E_0, and information about the pseudogap density of states (DOS), are determined, at low energies, from $\alpha(\hbar\omega)$-spectra.

Infrared (IR) transmission measurements were recorded on a PerkinElmer 580B double-beam spectrophotometer. The spectra were taken in the frequency range between 400 and 2200 cm^{-1} by placing a film (grown on roughened crystalline Si to eliminate interference fringes) in one beam and an identical bare substrate in the reference beam.

3. Results and discussion

3.1. Deposition kinetics

The empirical attempts at the optimization of a-$Si_{1-x}Ge_x$:H alloys have led to 'standard' conditions of low RF power and low gas pressure, which result in low deposition rates, r_d, of the order of 1 Å s^{-1} [21, 22]. Unfortunately a low deposition rate is considered to be a drawback in applications where a high throughput or thick films is desired. Therefore an increase of r_d in a-$Si_{1-x}Ge_x$:H film deposition is needed. Thus, many approaches have been tried in order to increase r_d without an increase of the spin density of the material, in the conventional RF discharge, such as the use of helium dilution instead of hydrogen. In particular, Hazra *et al* [23] have shown that r_d of optimized helium–diluted a-$Si_{1-x}Ge_x$:H material is 3.3 times greater than that of the hydrogen-diluted one with the same photoconductivities of both type of materials. Also, several works have proposed the advantage of replacing SiH_4 with Si_2H_6 in order to provide the plasma with species dissociating at closer rate to GeH_4. In this way, with very high H_2 dilution, Lundszein's group [24] has suggested that the deposition rate could be easily increased, without adverse effect on the material properties. With the same objective, and since the early work on helium dilution, important progress has been accomplished in the understanding of the RF discharge. In particular, it has been shown that r_d is mainly determined by the regime in which the discharge is sustained, and a significant increase of r_d can be observed when the discharge is operated in the high-pressure and high RF power regime. In this regime, the discharge becomes resistive and the RF energy is more efficiently coupled to the plasma through the bulk electrons which gain energy from the electric field produced in the inter-electrode space [25]. This is indeed verified here. Figure 1 presents the effect of the electrode gap on r_d (obtained from the ratio of the film thickness to the deposition time). It can be seen that r_d increases monotonically from 8.5 Å s^{-1} at $D = 0.8$ cm to 12 Å s^{-1} at $D = 3.2$ cm. The same trend has been observed by Harvard group on a-Ge:H films deposited also with variable electrode gap [18]. In agreement with these workers, we explain the large increase in the deposition rate by the increase of the negative potential of the cathode. As a consequence, more radicals are dissociated in the discharge, and the ions generated are accelerated across the dark sheath region to reach the cathode with a high sticking coefficient.

3.2. Hydrogen bonding and optical properties

Changes in the plasma chemistry at the grounded electrode, as D is varied, do not only affect the growth rate, but also the structure and the properties of the films. In order to determine the distribution of H between Si and Ge sites we used information from the IR hydrogen stretching

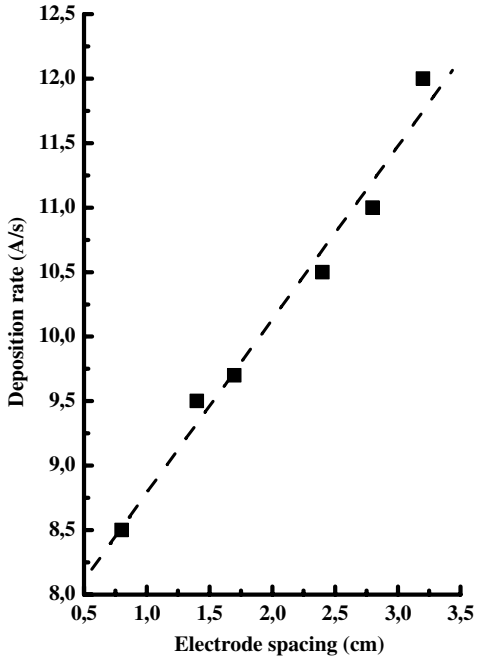

Figure 1. Deposition rate r_d as a function of electrode spacing.

vibration bands [13]. Figures 2(a)–(c) show the IR absorption spectra deposited at $D = 3.2$, 2.4 and 0.8 cm. In the high-frequency range, we used Gaussian line shapes centred around 1890 and 1975 cm^{-1} for Ge–H_n stretching modes ($n = 1, 2$), and around 2000 and 2090 cm^{-1} for Si–H_n ones. The areas under the Gaussians were used as adjustable parameters to obtain the best fit to the experimental IR spectra. From these figures it is seen clearly that:

- In the high-frequency range, and as D decreases, the areas corresponding to Ge–H and Si–H modes increase gradually while those corresponding to Ge–H_2 and Si–H_2 modes decrease. The spectrum corresponding to the sample deposited with the smaller D presents absorption bands at 1890 and 2000 cm^{-1} only. The stretch mode at 1890 cm^{-1}, associated with Ge–H entities, remains dominant. This means that, as D is decreased, hydrogen is mainly incorporated in the bulk of the material as Ge–H and Si–H groups, with a preferential attachment to Ge atoms over Si. The large absorption bands at 1975 and 2090 cm^{-1}, observed for the samples deposited with $D = 3.2$ and 2.4 cm, can be related to the distinct bending band consisting of two well-resolved peaks around 830 and 875 cm^{-1}, respectively. The presence of these bands indicates a significant proportion of $(Ge–H_2)_n$ and $(Si–H_2)_n$ complexes located at internal surfaces of voids, and these are often associated with deteriorated optoelectronic properties [26, 27]. With decreasing D, the bending modes decrease gradually and vanish for the lowest D value.

- In the low-frequency range, and as D decreases, the peak at 640 cm^{-1}, which corresponds to Si–H_n wagging mode, decreases slowly, while that at 560 cm^{-1}, which corresponds to the similar vibration modes of Ge–H_n bonds, increases.

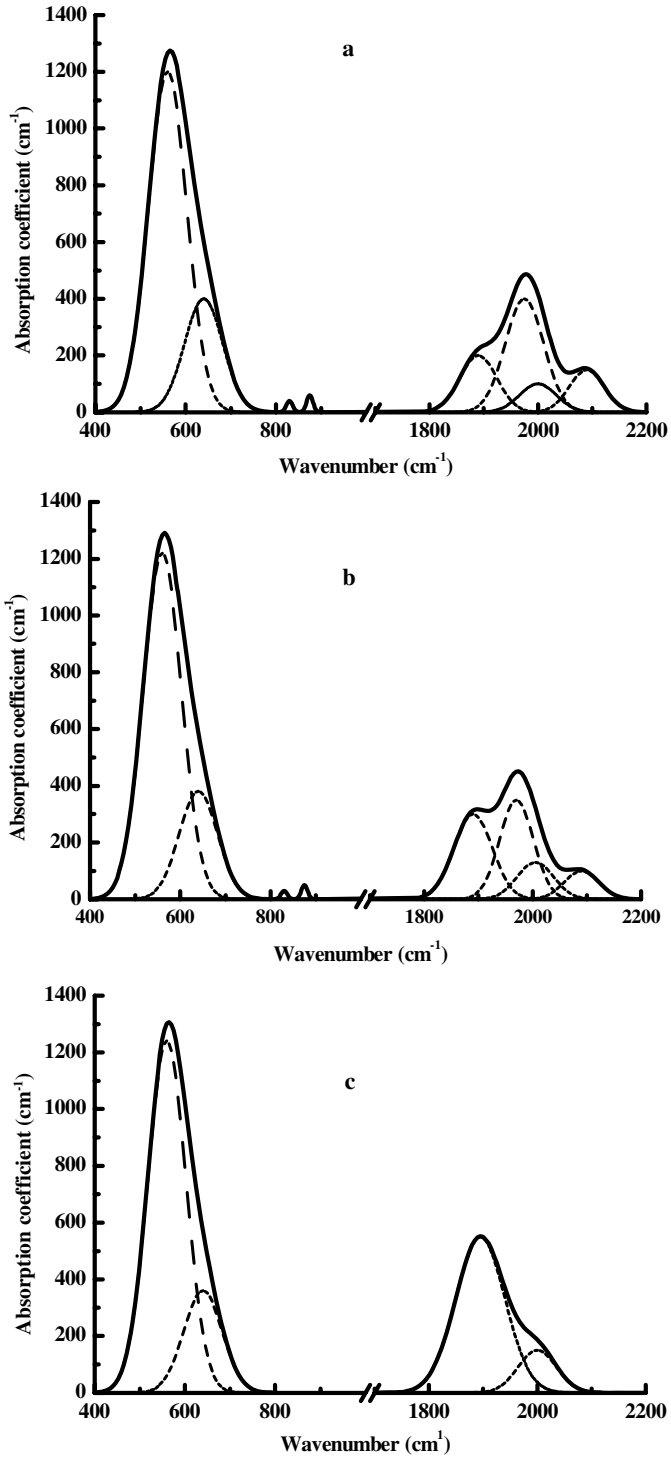

Figure 2. (a), (b), (c). Infrared absorption spectra for samples prepared using an electrode spacing of 3.2, 2.4 and 0.8 cm.

Table 1. Electrode spacing D. Deposition rate r_d obtained from the ratio of the film thickness to the deposition time. The microstructure parameter R deduced from infrared absorption spectra. The thickness d, the static refractive index n_0, the dispersion energy E_w, and the optical gap E_T, deduced from optical transmission measurements. The disorder parameter E_{0v}, and the absorption coefficient at 0.7 eV deduced from the PDS technique.

D (cm)	r_d (Å s^{-1})	R	d (μm)	n_0	E_w (eV)	E_T (eV)	E_{0v} (meV)	α (cm^{-1})
0.8	8.5	0	2.44	4.24	44	1.22	45	0.42
1.4	9.5	0.21	1.92	4.20	43	1.21	45	0.75
1.7	9.7	0.32	2.02	4.15	42	1.19	47	1.02
2.4	10.5	0.48	2.57	4.10	41	1.18	46	1.47
2.8	11	0.55	2.72	4.01	39	1.17	47	1.86
3.2	12	0.60	2.45	3.90	37	1.16	47	2.20

For structural characterization in a-Si$_{1-x}$Ge$_x$:H alloys, a combined microstructure parameter of both a-Si:H and a-Ge:H materials is often proposed [28]:

$$R = \frac{I^{\mathrm{Si}}_{2090} + I^{\mathrm{Ge}}_{1975}}{I^{\mathrm{Si}}_{2090} + I^{\mathrm{Si}}_{2000} + I^{\mathrm{Ge}}_{1975} + I^{\mathrm{Ge}}_{1890}} \tag{1}$$

where $I^{\mathrm{Si,\,Ge}}_{\omega}$ are the integrated areas under the absorption bands corresponding to Si–H$_n$ and Ge–H$_n$ stretching modes at frequency ω. This parameter has been shown to be related to the steady-state photoconductivity of a-Si:H films and related alloys [29]; also, a low microstructure parameter is often a sign of low void density material. The R values deduced from the spectra are summarized in table 1, and they suggest an improvement of the electronic properties of the material as D decreases.

Total hydrogen bond concentrations, C_H(at.%), were determined from the integrated areas, I_ω, of deconvoluted Gaussian curves fitted to IR absorption bands near 640 and 560 cm^{-1}. Following Cardona *et al* [30], the number of hydrogen bonds, N_H, is given by

$$N_H(\mathrm{cm}^{-3}) = A \int \frac{\alpha(\omega)}{\omega}\, \mathrm{d}\omega. \tag{2}$$

$\alpha(\omega)$ is the absorption coefficient of the film at frequency ω and A is the proportionality factor for these bands obtained by the calibration of N_H(cm^{-3}) against the hydrogen content deduced by the nuclear reaction technique; $A = 1.6\times10^{19}$ cm^{-2} for Si, and 1.1×10^{19} cm^{-2} for Ge [26].

C_H(at.%) was then obtained from the value of N_H:

$$C_H(\mathrm{at.\%}) = \frac{N_H(\mathrm{cm}^{-3})}{\rho_{\mathrm{Si,Ge}}} \times 100 \tag{3}$$

where $\rho_{\mathrm{Si,Ge}}$ is the atomic density of crystalline Si or Ge.

Hydrogen bond concentrations N(Ge–H), N(Ge–H$_2$), N(Si–H) and N(Si–H$_2$) were also determined from equation (2), by integration of deconvoluted bands due to Ge–H$_n$ and Si–H$_n$ ($n = 1, 2$) stretching modes. The values for the proportionality constant A used are, in cm^{-2},

$$A(\mathrm{Ge\text{–}H}) = 6\times10^{19}, \qquad A(\mathrm{Ge\text{–}H_2}) = 6\times10^{19} \text{ (see [31])}$$
$$A(\mathrm{Si\text{–}H}) = 1.2\times10^{20}, \qquad A(\mathrm{Si\text{–}H_2}) = 1.7\times10^{20} \text{ (see [32])}.$$

We checked in all cases that C_H(at.%) determined from the wagging modes is sensibly equal to that determined from the stretching ones. As expected, for fixed deposition temperature, the percentage of hydrogen remains constant at C_H(at.%) $\approx$ 8.5, for all the samples. The important point to note is the lowest value of C_H(at.%) obtained at normal growth temperature,

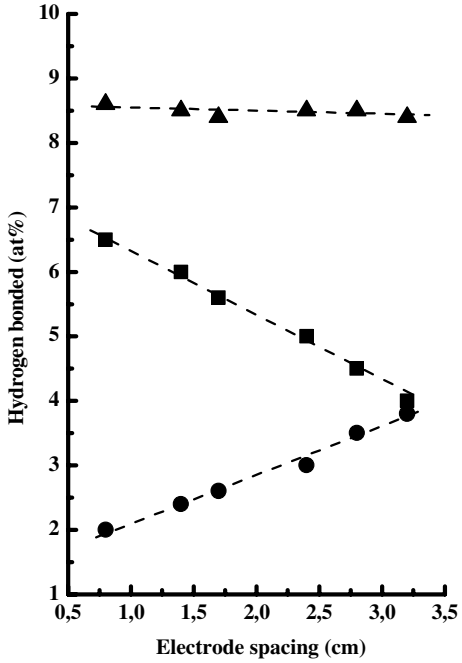

Figure 3. Hydrogen content in monoatomic form (Ge–H and Si–H bonds) (■), and in diatomic form (Ge–H_2 and Si–H_2 bonds) (●), as a function of electrode spacing. C_H (at.%) (▲) is also represented for completeness.

$T_s = 200\,^{\circ}C$, and high deposition rate. The variation of the electrode gap results only in a change in the distribution of H between Si and Ge sites. Figure 3 shows the hydrogen content strongly bonded to Ge and Si sites (Ge–H, and Si–H bonds), and the hydrogen content weakly bonded (Ge–H_2 and Si–H_2 bonds), as a function of D. It is seen clearly that, as D decreases, the hydrogen content that is strongly bonded is increased while that that is weakly bonded is decreased. The trends observed as D is varied must be correlated to significant changes in the microstructure and in the properties of the material.

To understand this phenomenon well, the Wemple–Didomenico one-oscillator model [33] is used to determine the static refractive index n_0, the average gap E_m, and the dispersion energy E_w:

$$n^2(\hbar\omega) = 1 + \frac{E_w E_m}{E_m^2 - (\hbar\omega)^2} \tag{4}$$

by considering the variation of $[n^2(\hbar\omega) - 1]^{-1}$ as function of $(\hbar\omega)^2$. The deduced values are summarized in table 1. The values of the optical band gap, E_T, determined by fitting the measured optical absorption coefficient α by the Tauc relation, $(\alpha\hbar\omega)^{1/2} = \mathrm{Cste}(E - E_T)$ [34], are also indicated in table 1 for completeness. Figure 4 shows a schematic band structure of the material and defines some parameters of this table. E_T decreases slowly from 1.22 eV at $D = 0.8$ cm to 1.16 eV at $D = 3.2$ cm. The average gap E_m, which is usually considered as the energy separation between the centres of both the conduction and the valence bands, did not follow the same trend, as we have reported in our previous work on a-Ge:H [19]; E_m remains practically constant at about 2.61 eV for all the samples. As it has been often reported [35], the band gap of a-$Si_{1-x}Ge_x$:H alloys is affected by three factors: the total bonded hydrogen content, composition x and hydrogen-bonding configurations. All these factors have

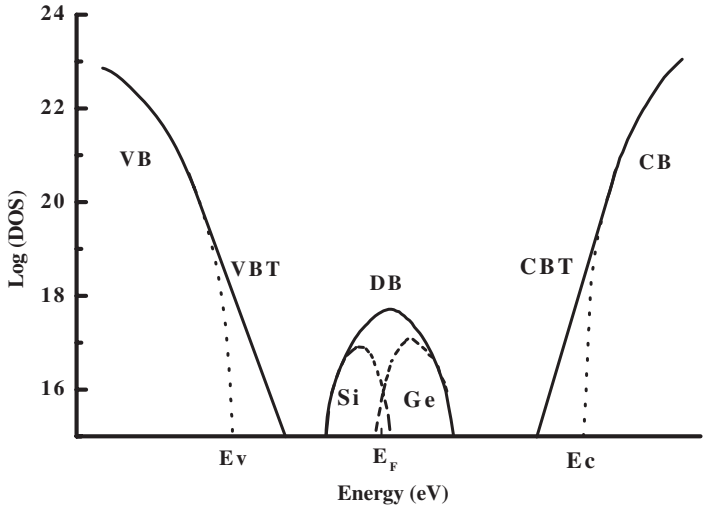

Figure 4. Schematic band structure for a-$Si_{1-x}Ge_x$:H showing the location of the Si and Ge dangling-bond centres with respect to the conduction and valence bands (CB and VB). The conduction and the valence bandtails (CBT and CVT) are described by exponential distributions with width E_{ov} and E_{oc}, respectively. $E_T = E_c - E_v$ defines the optical gap.

been examined by several authors [36], but ambiguities remain in distinguishing the effects of their variations on the bandgap, and quantitative information is difficult to obtain. In this study, the first two factors were constant for all the samples; we try to examine the effect of the last one on the bandgap. Figure 5 shows the variation of E_T as a function of the content of hydrogen singly bonded to Ge and to Si sites. No similar variations were observed with other hydrogen-bonding configurations. From this trend it appears clearly that the change in the proportion of hydrogen strongly bonded to Ge and to Si atoms affects E_T (i.e. the energy separation between the extrema of both the conduction and the valence bands), and must be attributed to an explicit alloying effect between the atoms of Ge and H, and between the atoms of Si and H, respectively. Since the composition x of Ge and C_H(at.%) remain constant for all samples, we speculate that this effect is not enough to affect the centres of the conduction and the valence bands.

In order to examine the effect of the hydrogen-bonding configurations on the microstructure of the material, we determine the static refractive index n_0, which is often related to the optical gap, to the material density, or to both of them. As seen in table 1, n_0 shows a decrease from 4.24 to 3.90 when E_T is decreased. This trend is in disagreement with the prediction of the model proposed by Penn [37], which suggests an increase of n_0 values when the bandgap is decreased. The values of the dispersion energy E_w show the same variations as n_0, and suggest a decrease in the average coordination number of the atoms. So, we attribute the diminution of n_0 values, as D is increased, to a small amount of microstructure and to a small density loss in the material. Figure 6 shows the variation of n_0 as a function of the microstructure parameter R. These trends suggest that the inhomogeneous structure which appears in the material, as D is increased, must be attributed to the incorporation of the hydrogen as Ge–H_2 and Si–H_2 groups in the bulk of the material. But the values of n_0 and E_w remain high in all of the range of D variation, and suggest that the particular microstructure of the films is not of the 'island and tissue' type [38] but may rather consist in a dense matrix with small isolated voids within the network with a low hydrogen content.

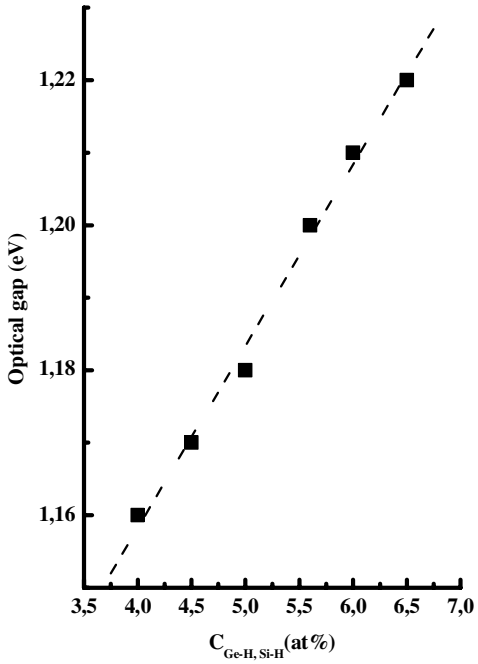

Figure 5. Optical gap as a function of the content of hydrogen bonded to Ge and to Si in monoatomic form.

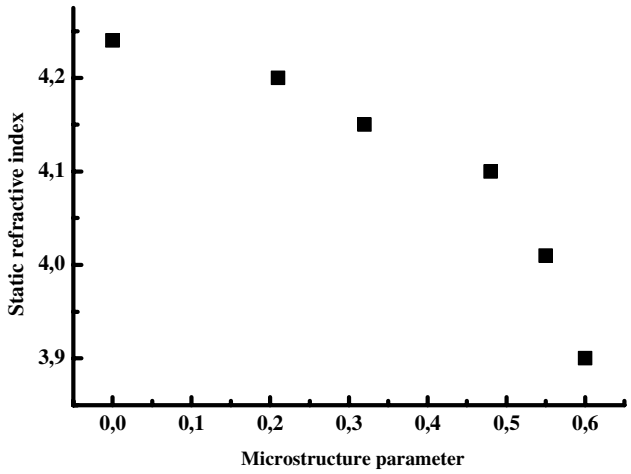

Figure 6. Static refractive index as a function of the microstructure parameter.

3.3. Subgap absorption

Here we analyse the effects of the gap electrode on the optical absorption spectra obtained as explained before from a combination of optical transmission and PDS experiments. All the samples were studied in their as-deposited state. The PDS spectra were normalized to absolute values by matching the Urbach edge region with the optical absorptance spectra deduced from optical measurements in the high-energy range [39]. The optical absorption spectra $\alpha(\hbar\omega)$

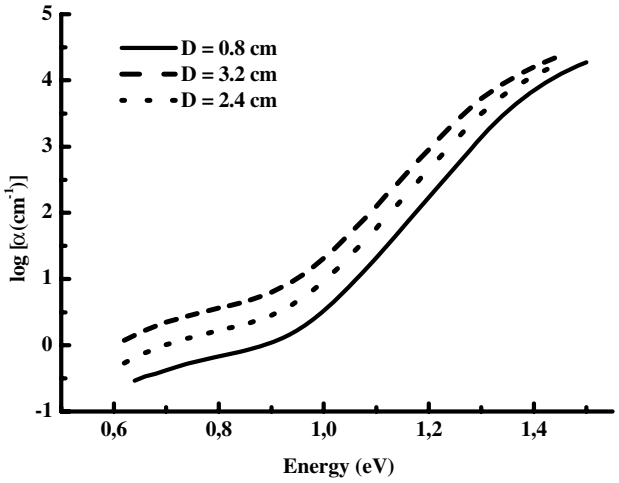

Figure 7. Absorption spectra deduced from the PDS and standard transmission techniques for samples deposited at different electrode gap spacing: $D = 3.2$, 2.4 and 0.8 cm.

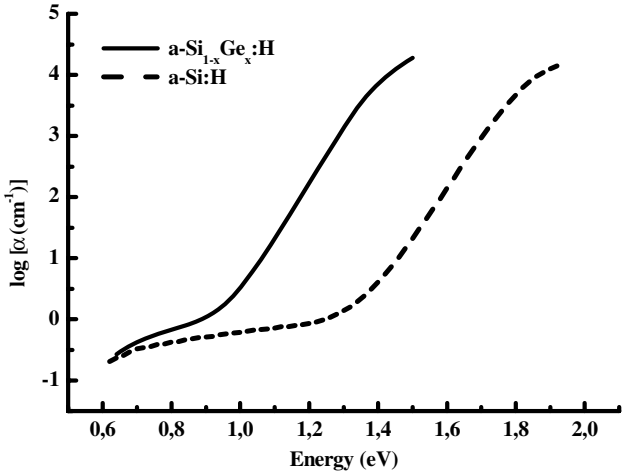

Figure 8. Optical absorption coefficient spectrum of a-$Si_{1-x}Ge_x$:H film prepared using an electrode spacing of 0.8 cm, compared to that of device-quality a-Si:H, deposited by the PECVD technique at a low deposition rate ($r_d = 1$ Å s^{-1}) in the 'standard' conditions (low RF power: 10 W, low pressure: 40 mTorr, and at a substrate temperature of 200 °C).

are then deduced from the ratio of the normalized PDS spectra to the transmittance ones, as suggested by our procedure [40]. The spectra obtained are displayed in figure 7. With decreasing D the absorption edge shifts towards higher energies, with a concurrent decrease in the low-energy range. This effect is obviously related to the hydrogen-bonding configurations, and mainly to the increase of the hydrogen content singly bonded to Ge and to Si sites in the bulk of the material. The important remarks which can be made about these spectra are their lower levels of absorption at lower energies, and their sharp edges in the exponential range. Thus, for example in figure 8, the spectrum of the optimized a-$Si_{1-x}Ge_x$:H film is compared to that of device-quality a-Si:H film, deposited by the PECVD technique in the 'standard' conditions at low deposition rate ($r_d \sim 1$ Å s^{-1}).

Some characteristic parameters can be derived from the analysis of these spectra. For energies lower than the optical gap, $\alpha(\hbar\omega)$ provides useful information about the pseudogap density of states (DOS). On the one hand, the inverse slope of the exponential part of the edge, E_0 (Urbach energy), can be considered equal to the width of the valence bandtail E_{0v}, and it characterizes the disorder and the distorted or the weak bonds. On the other hand, the level of absorption at energies below the Urbach tail is determined by the deep-gap state density N_D. The Urbach energy is usually determined by a linear regression of the exponential data range. However, the contribution of the deep-defect absorption in this range may increase this parameter, in particular for the non-optimized samples. In previous works [19, 41], we have shown, by considering a suitable deconvolution of $\alpha(\hbar\omega)$ applied to a-Ge:H films, that E_{0v} values obtained by this procedure differ by only about 1–2 meV for the optimized samples, and by about 12 meV for the worst samples, from those determined by a linear regression. So, for $\alpha(\hbar\omega)$ spectra with a low absorption level, such as those presented in figure 7, a deconvolution procedure (based always on some assumptions) is not necessary to determine E_{0v}. The apparent values are not much influenced by the contribution of the deep-gap state absorption in the Urbach-tail range. So, in this work, E_{0v} values were deduced by a linear regression of the exponential range, and they are summarized in table 1. These values show no significant dependence on D, and are of the same order as those of device-quality a-Si:H film ($E_{0v} \approx 50$ meV).

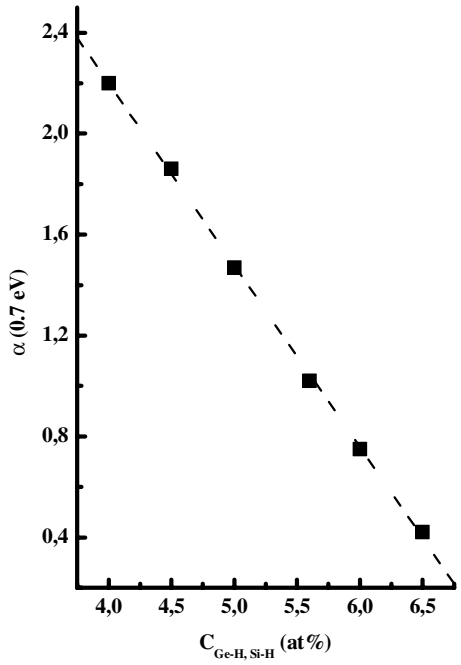

Figure 9. Variation of the optical absorption coefficient at 0.7 eV versus the hydrogen content in monoatomic form (Ge–H and Si–H bonds).

Various methods have been proposed to estimate N_D, or to obtain information on the DOS via $\alpha(\hbar\omega)$ spectra, either by some calibration procedure [42], by fitting these spectra with a model of DOS [43], or by their derivation with respect to energy [44]. All methods, however, are based on certain simplifying assumptions and are matter of discussion. Thus, it has been a convention for a-Ge:H material to use the value of absorption coefficient

around the midgap energy α (0.6–0.7 eV) as a parameter characterizing the deep-defect absorption [16, 17]. In particular, for a-Ge:H we have shown that a good linear correlation is observed between the density of spin determined by electronic paramagnetic resonance and α (0.6 eV) [45], and between the deep-defect density, estimated by a deconvolution procedure, and the corresponding α (0.7 eV) values [41]. The subgap absorption, α (0.7 eV), deduced from PDS spectra are summarized in table 1. With decreasing D, α (0.7 eV) values decrease slowly and reach an optimum value (α (0.7 eV) $= 0.42$ cm^{-1}) for the sample deposited at lower D.

Already, it has been reported that the deterioration of the electronic quality of a-$Si_{1-x}Ge_x$:H alloys, with high Ge content, is mainly attributed to the preferential attachment of hydrogen to Si atoms. Here, we suggest that the remarkable improvement of the quality of the alloy is mainly due to the increase of the hydrogen incorporated as monohydride form, with a preferential attachment to Ge. By simply reducing the electrode gap spacing, the monohydride bond dominates instead of the polyhydride, and consequently the microvoids, network distortion and dangling bonds reduce. Figure 9 is in perfect agreement with this suggestion, since the plot of α (0.7 eV) versus the corresponding content of hydrogen incorporated as monohydride bonds (Ge–H, Si–H) shows a good linear correlation. This explanation is in good agreement with that proposed recently by Liu *et al* [46], who have been able to make, by using a very low pressure electron cyclotron resonance (ECR) plasma deposition, good-quality a-$Si_{1-x}Ge_x$:H material with significant Ge–H bonds in addition to Si–H bonds and an absence of polyhydride forms, which represent a clustered H microstructure.

4. Summary and conclusion

As a conclusion, this experimental work brings new results for understanding the effects of the hydrogen on the structural and optoelectronic properties of a-$Si_{1-x}Ge_x$:H films deposited at high growth rate by RF glow discharge. The following conclusions can be drawn from this study.

- As D was varied, a gradual change in the hydrogen-bonding configurations was observed. As a consequence, a continuous change in both the structural and the optoelectronic properties appears in the material.
- As D was decreased, the hydrogen was gradually incorporated in the bulk of the material in the monoatomic form, with a preferential attachment to Ge atoms. The total hydrogen bond concentrations is constant with D: C_H (at.%) ≈ 8.5.
- The films are of large Ge composition, their optical gaps, E_T, are less than those of conventional films, reported in the literature [7, 8]. A good linear correlation between E_T and the total hydrogen content in monoatomic form (Ge–H and Si–H bonds) is observed: there is an explicit alloying effect between the atoms of Ge and H, and between the atoms of Si and H, respectively. But, no similar effect was observed on the average gap, E_m.
- Changes observed in both the static refractive index, n_0, and in the dispersion energy, E_W, as D was increased, are related to the appearance of a small amount microstructure and to a small density loss in the material, mainly attributed to Ge–H_2 and Si–H_2 entities.
- The remarkable improvement in the defect density and in the disorder parameter, as D is decreased, is attributed to the incorporation of the hydrogen in the bulk of the material as Ge–H and Si–H bonds, with a preferential attachment to Ge sites.
- The absorption level and the disorder parameter of optimized samples are of the same order as those of device-quality a-Si:H films.

Acknowledgments

We wish to thank Dr M L Thèye for many helpful discussions and Professor W Paul for providing the samples used in this study.

References

[1] Dalal V L 2002 *Curr. Opin. Solid State Mater. Sci.* **6** 455
[2] Palinginis K C, Cohen J D, Yang J C and Guha S 2000 *J. Non-Cryst. Solids* **266–269** 665
[3] Tzoumanekas C and Kelires P C 2000 *J. Non-Cryst. Solids* **266–269** 670
[4] Arya R 2000 *Proc. Conf. on 28th IEEE Photovoltaic. Spec.* p 19
[5] Okamoto S, Terakawa A, Maruyama E, Shinohara W, Hishikawa T and Kiyama S 2000 *Proc. Conf. on 28th IEEE. Photovoltaic. Spec.* p 736
[6] Chou Y P and Lee S C 1998 *J. Appl. Phys.* **83** 4111
[7] Shima M, Terakawa A, Isomura M, Haku H, Tanaka M, Wakisaka K, Kiyama S and Tsuda S 1998 *J. Non-Cryst. Solids* **227–230** 442
[8] Soukup R J, Ianno N J, Darveau S A and Extrom C L 2005 *Sol. Energy Mater. Sol. Cells* **87** 87
[9] Wagner S, Chu V, Chen D S, Conde J P, Aljishi S and Smith Z E 1988 *Mater. Res. Soc. Symp. Proc.* vol 118 (Pittsburgh, PA: Materials Research Society) p 623
[10] Jones S J, Chen Y, Williamson D L, Zedlitz R and Bauer G 1993 *Appl. Phys. Lett.* **62** 3267
[11] Aljishi S, Smith Z E, Slobodin D, Kolodzey J, Chu V, Schwarz R and Wagner S 1986 *Mater. Res. Soc. Symp.* **7** 269
[12] Weisz S Z, Gomez M, Muir J A, Resto O, Goldstein Y and Ables B 1984 *Appl. Phys. Lett.* **52** 634
[13] Paul W, Paul D K, Roerden B V, Blake J and Oguz O 1981 *Phys. Rev. Lett.* **46** 1016
[14] Mackenzie K D, Eggert J R, Leopold D L, Li Y M, Lin S and Paul W 1985 *Phys. Rev.* B **31** 2198
[15] Godet C, Chu V, Equer B, Bouizem Y, Chahed L, El Zawawi I, Thèye M L, Basrour S, Bruyère J C and Stoquert J P 1990 *Mater. Res. Soc. Symp.* **192** 163
[16] Wetsel A E, Jones S J, Turner W A, Pang D, Paul W, El Zawawi I, Bouizem Y, Chahed L, Thèye M L, Marques F C and Chambouleyron I 1990 *Mater. Res. Soc. Symp.* **192** 547
[17] Turner W A, Jones S J, Pang D, Bateman B F, Chen J H, Li Y M, Marques F C, Wetsel A E, Wickboldt P, Paul W, Bodart J, Norberg R E, El Zawawi I and Thèye M L 1990 *J. Appl. Phys.* **67** 7430
[18] Wickboldt P, Jones S J, Pang D, Turner W A, Wetsel A E, Paul W and Chen J H 1991 *Phil. Mag.* B **64** 655
[19] Bouizem Y, Belfedal A, Sib J D, Kebab A and Chahed L 2005 *J. Phys.: Condens. Matter* **17** 5149
[20] Amer N M and Jackson W B 1984 *Semiconductors and Semimetals* vol 21B, ed J I Pankove (New York: Academic) p 83
[21] Dalal V, Haroon S, Zhou Z, Maxson T and Han K 2000 *J. Non-Cryst. Solids* **266–269** 675
[22] Middya A R and Ray S 1994 *J. Appl. Phys.* **75** 7340
[23] Hazra S, Middya A R and Ray S 1996 *J. Non-Cryst. Solids* **211** 22
[24] Lundszein D, Fölsch J, Finger F and Wagner S 1997 *Proc. 14th European PV Solar Energy Conf. (Barcelona)* p 578
[25] Bohm C and Perrin J 1991 *J. Phys. D: Appl. Phys.* **24** 865
[26] Bermejo D and Cardona M 1979 *J. Non-Cryst. Sol.* **32** 421
[27] Freeman E C and Paul W 1978 *Phys. Rev.* B **18** 4288
[28] Abo Ghazla M S 2000 *Physica* B **293** 132
[29] Bhattacharya E and Mahan A H 1988 *Appl. Phys. Lett.* **52** 1587
[30] Cardona M 1983 *Phys. Status Solidi* b **118** 463
[31] Shima M, Terakawa A, Isomura M, Tanaka M and Tsuda S 1995 *Proc. 13th European PV Solar Energy Conf. (Nice)* p 269
[32] Langford A, Fleet M, Nelson B, Lanford W and Maley N 1992 *Phys. Rev.* B **45** 13367
[33] Wemple S H and Didomenico M 1971 *Phys. Rev.* B **3** 1338
[34] Tauc J 1974 *Amorphous and Liquid Semiconductors* (New York: Plenum) chapter 4
[35] Roedern B V, Paul D K, Blake J, Collins R W, Moddel G and Paul W 1982 *Phys. Rev.* B **25** 7678
[36] Maley N and Lannin J 1987 *Phys. Rev.* B **36** 1146
[37] Penn D R 1962 *Phys. Rev.* B **128** 2098
[38] Paul W 1988 *Amorphous Silicon and Related Materials* vol 1A, ed H Fritsche (Singapore: World Scientific) p 63
[39] Thèye M L, Chahed L, Rocca i Cabarrocas P and Zellama K 1991 *Phil. Mag.* B **63** 143
[40] Bouizem Y, Belfedal A, Sib J D and Chahed L 2000 *Opt. Commun.* **178** 111

[41] Bouizem Y, Belfedal A, Sib J D and Chahed L 2003 *Solid State Commun.* **126** 675
[42] Jackson W B and Amer N M 1982 *Phys. Rev.* B **25** 5559
[43] Triska A, Kocka J and Vanecek P l 1987 *Disordered Semiconductors* ed A Kastner, G A Thomas and S R Ovshinsky (New York: Plenum) p 459
[44] Jensen P 1990 *Solid State Commun.* **76** 1301
[45] Godet C, Bouizem Y, Chahed L, El Zawawi I, Thèye M L, Meaudre M, Meaudre R, Basrour S and Bruyère J C 1991 *Phys. Rev.* B **44** 5506
[46] Liu Y and Dalal V 2002 *Proc. Mater. Res. Soc.* **715** A18.3